Lawrence Berkeley Laboratory

UNIVERSITY OF CALIFORNIA
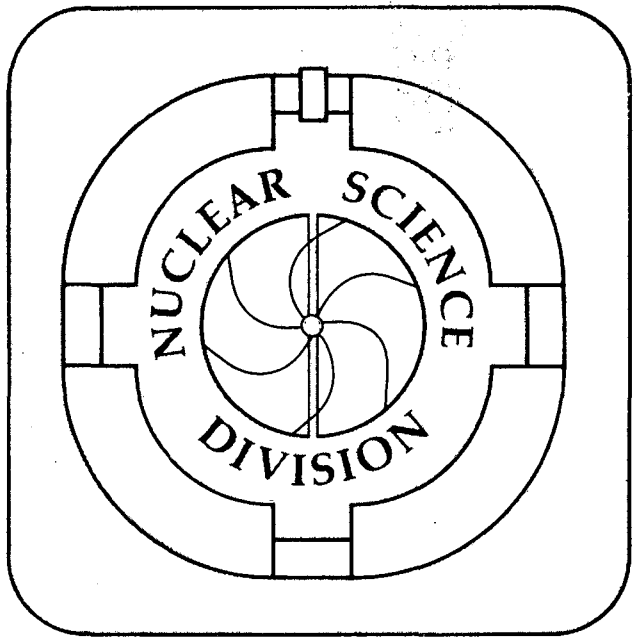
Incomplete Fusion and Complex Fragment Emission: A Continuum of Isotropic Sources

N. Colonna, R.J. Charity, D.R. Bowman, M.A. McMahan,
G.J. Wozniak, L.G. Moretto, G. Guarino, A Pantaleo,
L. Fiore, A. Gobbi, and K.D. Hildenbrand

December 1988

DISCLAIMER

Incomplete Fusion and Complex Fragment Emission:
A Continuum of Isotropic Sources.

N. Colonna, R. J. Charity,[1] D. R. Bowman, M. A. McMahan, G. J. Wozniak,
and L. G. Moretto

*Nuclear Science Division, Lawrence Berkeley Laboratory, 1 Cyclotron Rd., Berkeley, California
94720, USA*

G. Guarino, A. Pantaleo and L. Fiore

Istituto Nazionale di Fisica Nucleare INFN, Sezione di Bari, 70126 Bari, Italy

A. Gobbi and K. D. Hildenbrand

Gessellschaft für Schwerionenforschung, 6100 Darmstadt, West Germany

Abstract:

When observed in singles, complex fragments associated with the 18 A MeV ^{139}La +
^{64}Ni reaction present a complex invariant cross section pattern without an obvious
source, while the center-of-mass velocities of the coincident binary events span the
entire range from complete fusion to near projectile velocities. By gating on a given
value of the source velocity, it is possible to characterize precisely the product formed
in the corresponding incomplete-fusion process and its decay.

[1]Present address: Gessellschaft für Schwerionenforschung, 6100 Darmstadt, West Germany

Two fundamental problems are associated with complex fragment emission at intermediate energies. The first is the discovery and characterization of the possible sources, the second is the mechanism involved in their formation.

In many experiments the picture is very complicated and the lack of simple source patterns has led to a proliferation of speculations and misconceptions. The complexity of these reactions seems to arise from the fact that the reaction mechanism depends as much on the mass asymmetry of the entrance channel as on bombarding energy.

Fortunately, very asymmetric target-projectile combinations lead to the formation of a simple source pattern, a circular Coulomb ring, easily identifiable in reverse kinematics. Studies[1-9] of these systems have led to the identification of the compound nucleus as an important source of complex fragments formed in binary decays at all exit channel asymmetries. In addition, quasi and deep inelastic processes are responsible for fragment production in the vicinity of the target and projectile. These compound nuclei are formed in complete or incomplete fusion processes, depending on the entrance channel asymmetry and on the bombarding energy. Simple source patterns are produced at low energy because of the dominance of complete fusion.[4-6] At higher energies[8-10], when incomplete fusion sets in, the source pattern remains simple because of an intricate interplay between incomplete fusion and complex fragment decay probability, through their dependence upon impact parameter.[10]

This simple source pattern disappears in more symmetric systems. This may be caused by the increased range of impact parameters, and by the associated incomplete-fusion process. However, the lessons that we have learned from the very asymmetric systems may help unravel the puzzle.

We shall show in this Letter that the only substantive change occuring in more symmetric systems is the formation of a continuous range of sources associated with the full range of incomplete fusion processes. These sources have a continuum of velocities, total masses, and excitation energies, but in all other respects they resemble

the fusion products formed in more asymmetric systems, and decay in a similar way. This will be demonstrated in the reaction ^{139}La + ^{64}Ni at 18 A MeV, for which we have determined the distribution of source velocities, established their mass and excitation energy, and demonstrated the consistency of the missing charge with evaporation from the hot fragments.

A beam of 18 A MeV ^{139}La from the Gesellschaft für Schwerionenforschung UNILAC bombarded a 1.1 mg/cm^2 ^{64}Ni target. Reaction products were detected with two position-sensitive quad ΔE-E telescopes placed symmetrically on opposite sides of the beam. The energy loss was measured with a gas ionization chamber (ΔE) operated with CF$_4$ and the residual energy was measured with a 5 mm thick Li-drifted Si detector. Individual peaks were observed for atomic numbers up to $Z = 35$ and fragments were identified up to $Z = 59$ with an uncertainty of about one charge unit. The solid state detectors had an active area of 4.6x4.6 cm^2 and were position-sensitive in the horizontal dimension. The vertical coordinate was determined from the drift time in the ionization chamber. The position resolution was 2 mm, which corresponds to 0.2^o. These detectors covered 20° in plane and 5° degrees out-of-plane. Elastic scattering of ^{139}La + ^{197}Au and fission fragments from a ^{252}Cf source were used to calibrate the telescopes. The energy calibration was accurate to within 2% over the entire fragment mass range.

The mass of a fragment was inferred from its measured charge as described in Ref. 5. The velocity of a fragment was calculated from its measured energy and inferred mass. For binary coincidences in which one fragment has the atomic number $Z = 30$, the cross section $\partial^2\sigma/\partial v_{\parallel}\partial v_{\perp}$ in the $v_{\parallel}$ - $v_{\perp}$ plane is shown in Fig. 1b. In this display, one observes an elliptical pattern stretched along the beam direction. Although a high degree of relaxation can be inferred, it is not possible to associate these events with a single source. For comparison, a more asymmetric reaction like ^{139}La + ^{12}C (see Fig. 1a) shows a sharp isotropic Coulomb circle indicating the presence of a single source

with a well defined velocity. The Z_1-Z_2 correlation diagram for the ^{139}La + ^{64}Ni reaction (Fig. 1g) is very broad whereas the one for the ^{139}La + ^{12}C reaction (Fig. 1f) is much narrower.

The cause of these "anomalous" features becomes apparent when the velocity spectrum of the centers of mass of the coincident fragments is determined. This spectrum is shown in Fig. 2 for three reactions: 18 A MeV ^{139}La + ^{12}C, ^{27}Al and ^{64}Ni. For the very asymmetric ^{139}La + ^{12}C , ^{27}Al systems, the center-of-mass velocity spectra show single sharp peaks. These peaks correspond to the velocities of the centers-of-mass of the entire system and they indicate the absence of a third body. The total relaxation of the kinetic energies, mass and angular distributions allows us to attribute these peaks to a complete fusion process. For the more symmetric ^{139}La + ^{64}Ni reaction, one observes a similar peak, that we also attribute to complete fusion, plus an additional shoulder that stretches out to velocities approaching that of the projectile. This high velocity shoulder indicates the presence of a third body associated with a continuum of incomplete fusion processes extending over the entire allowed mass range.

Of course, caution must be exercised in interpreting this curve as the "true" distribution in source velocities. On the one hand, the peak can contains all kinds of two body decays, in particular deep-inelastic decay. On the other, the measured distribution may be biased (though not seriously) by the coincidence efficiency of our apparatus, and the velocity spectrum is broadened by the light particle evaporation, which may either precede or follow the complex fragment decay.

Despite these possible biases, the measured source velocity distribution can be used to unravel the complexity of the ^{139}La + ^{64}Ni reaction by selecting events with well defined source velocities. For example, in Fig. 1(c, d, & e), the velocity plots for Z = 30, are gated on three different velocity bins, namely the velocity corresponding to complete fusion velocity, 50% fusion and 25% fusion. These three velocity plots now

display isotropic circular patterns similar to the Coulomb circles seen in the very asymmetric systems, but <u>with their centers progessively shifted towards higher values of $v_{||}$</u>. There is also a striking decrease in the radii of these Coulomb circles with increasing source velocities. This correlation occurs since, as the projectile picks up more mass from the target, its velocity decreases. The complex fragment is thus emitted from a heavier and slower source. In addition, as the total charge of the source decreases, the Coulomb velocity associated with a fixed fragment Z value decreases, because the splitting becomes more symmetric.

The ungated Z_1-Z_2 correlation diagram as well as those gated on the same velocity bins are also shown in Fig. 1. The broad ungated distribution (see Fig. 1g) indicates a broad distribution in the total charge of the source due to the extended range of incomplete fusion. By restricting the source velocity, this broad distribution is decomposed into three narrower correlation diagrams (see Fig. 1h, i, j), with the characteristic pattern observed for very asymmetric systems like ^{139}La + ^{12}C (see Fig. 1f). As the source velocity increases, the diagonal pattern shifts from larger to smaller total Z values. The greatest average sum of the fragment atomic numbers $<Z_1 + Z_2>$ occurs for the complete fusion velocity. The quantity $<Z_1 + Z_2>$ decreases with increasing source velocity, which corresponds to progressively less extensive fusion of the target with the projectile. Thus, the broad ungated correlation diagram observed in Fig. 1g, can be decomposed into a series of narrower patterns, by setting gates on the source velocity.

The observed atomic numbers of the coincident fragments are those resulting after evaporation from either the hot compound nucleus, or the hot primary fragments resulting from its binary decay. It would be useful to obtain information on their primary atomic numbers. One can estimate the total primary charge of the incomplete fusion product from the corresponding source velocity, namely:

$$Z_{IF} \cong Z_P V_P / V_{IF} \tag{1}$$

Similarly, one can estimate the excitation energy of the incomplete fusion product:

$$E_x (IF) \cong E_x (CF) \frac{V_P - V_{IF}}{V_P - V_{CF}} . \qquad (2)$$

For complete fusion, one obtains $E_x \sim 800$ MeV for the compound nucleus ^{205}At, which corresponds to 4 MeV/nucleon and a temperature of 6.5 MeV. While higher temperatures have been advocated from spectral slopes or particle multiplicities, this may well be the highest temperature that can be firmly associated with a well characterized system.

One should be aware that light particle evaporation causes some uncertainty in these estimatied quantities. With this caution in mind, one can plot the difference between the estimated primary charge and the measured average secondary charge as a function of the estimated excitation energy (see Fig. 3). The approximate linearity of the plot is consistent with the evaporation hypothesis. A more quantitative check can be made by assuming that the binary decay occurs first, and that all of the remaining excitation energy is disposed of by evaporation from the two fragments. The angular momentum of the fragment, needed for the evaporation calculation, was estimated from a two sphere scission configuration. The maximum partial wave leading to complete fusion was calculated with the Bass model[11], while in the case of incomplete fusion the model of Ref. 12 was used.

The results obtained from the evaporation code PACE are shown in the same figure. Given the very rough assumptions of equations 1 & 2 and the crude estimate of the angular momentum of the fragments, the agreement between the data and the calculations is quite satisfactory.

In light of the above discussion, we can describe the 18 A MeV ^{139}La + ^{64}Ni reaction as follows: 1) The events associated with the "complete fusion peak" arise from either compound nucleus binary decay of the complete fusion object, or from quasifission binary decay, or, possibly, from (quasi) deep inelastic reactions. 2) The

events associated with the higher velocity components are essentially ternary incomplete fusion events. The target-like spectator, observable in singles[5-10] as part of the low velocity "big foot" is not detected in coincidence. The forward moving incomplete fusion products, whose masses are smaller the faster their velocities, give rise to the observed continuum of complex fragment sources. 3) If the incomplete fusion product undergoes a binary decay, this continuum can be analyzed by reconstructing the source velocity from the two coincident heavy fragments.

It is clear that other more symmetric systems could be studied in a similar fashion.

From the analysis of the present moderately symmetric system, we conclude that the processes involved in complex fragment formation, in this energy regime, are no different than those present in more asymmetric systems. The only complicating feature is the broad range of incompete fusion products, resulting in a broad range of source velocities. Perhaps this conclusion will apply for symmetric systems and even higher bombarding energies. In any event, we have demonstrated a novel technique for studying, in a single reaction system, the decay properties of a wide range of compound nuclei with a continuous range of excitation energies.

Acknowledgements

References

1. L. G. Moretto and G. J. Wozniak, Prog. in Part. & Nucl. Phys. **21** (1988) 401.

2. L. G. Sobotka et al., Phys. Rev. Lett. **51** (1983) 2187.

3. M. A. McMahan et al., Phys. Rev. Lett. **54** (1985) 1995.

4. L. G. Sobotka et al., Phys. Rev. Lett. **53** (1984) 2004.

5. R. J. Charity et al., Nucl. Phys. **A483** (1988) 371.

6. H. Han et al., Lawrence Berkeley Laboratory preprint # LBL-25743 (1988).

7. E. Plagnol et al., Lawrence Berkeley Laboratory preprint # LBL-25742 (1988).

8. R. J. Charity et al., Phys. Rev. Lett. **56** (1986) 1354.

9. D. R. Bowman et al., Phys. Lett. **B189** (1987) 282.

10. R. J. Charity et al., Nucl. Phys. **A476** (1988) 516.

11. R. Bass, Phys. Rev. Lett. **39** (1977) 265.

12. L. G. Moretto and D. R. Bowman, Proc. of the XXIV Int'l Winter Meeting on Nucl. Phys., Bormio, Italy, Jan. 20 -25, 1986, Ricerca Scientifica ed. Educazione Permanente, Suppl. N. **49** (1986) 126.

Figure Captions

Fig. 1 Contour diagrams of invariant cross section in the $V_{||}$ - $V_{\perp}$ plane (left column) and Z_1 - Z_2 (right column) for Z = 30 fragments from the 18 A MeV ^{139}La + ^{12}C reaction (first row) and for the 18 A MeV ^{139}La + ^{64}Ni reaction. Various gating conditions on the source velocity are indicated to the left of each row. The horizontal arrows indicate the magnitude of the source velocity and the diagonal dashed lines indicate the atomic numbers of the projectile and of the fused system as inferred from the source velocity.

Fig. 2 Source velocity distributions for the 18 A MeV ^{139}La + ^{12}C, ^{27}Al, ^{64}Ni reactions as extracted from the binary coincidences (see text). The vertical arrows indicate the velocities corresponding to complete fusion for the three reactions.

Fig. 3 The measured evaporated charge (dots) plotted versus the excitation energy determined from the source velocities for the 18 A MeV ^{139}La + ^{64}Ni reaction. The horizontal and vertical bars on each data point reflect the width of the bin in the source velcity from which the primary charge and the excitation energy of the incomplete fusion product was extracted. The solid line was calculated with the evaporation code PACE (see text).
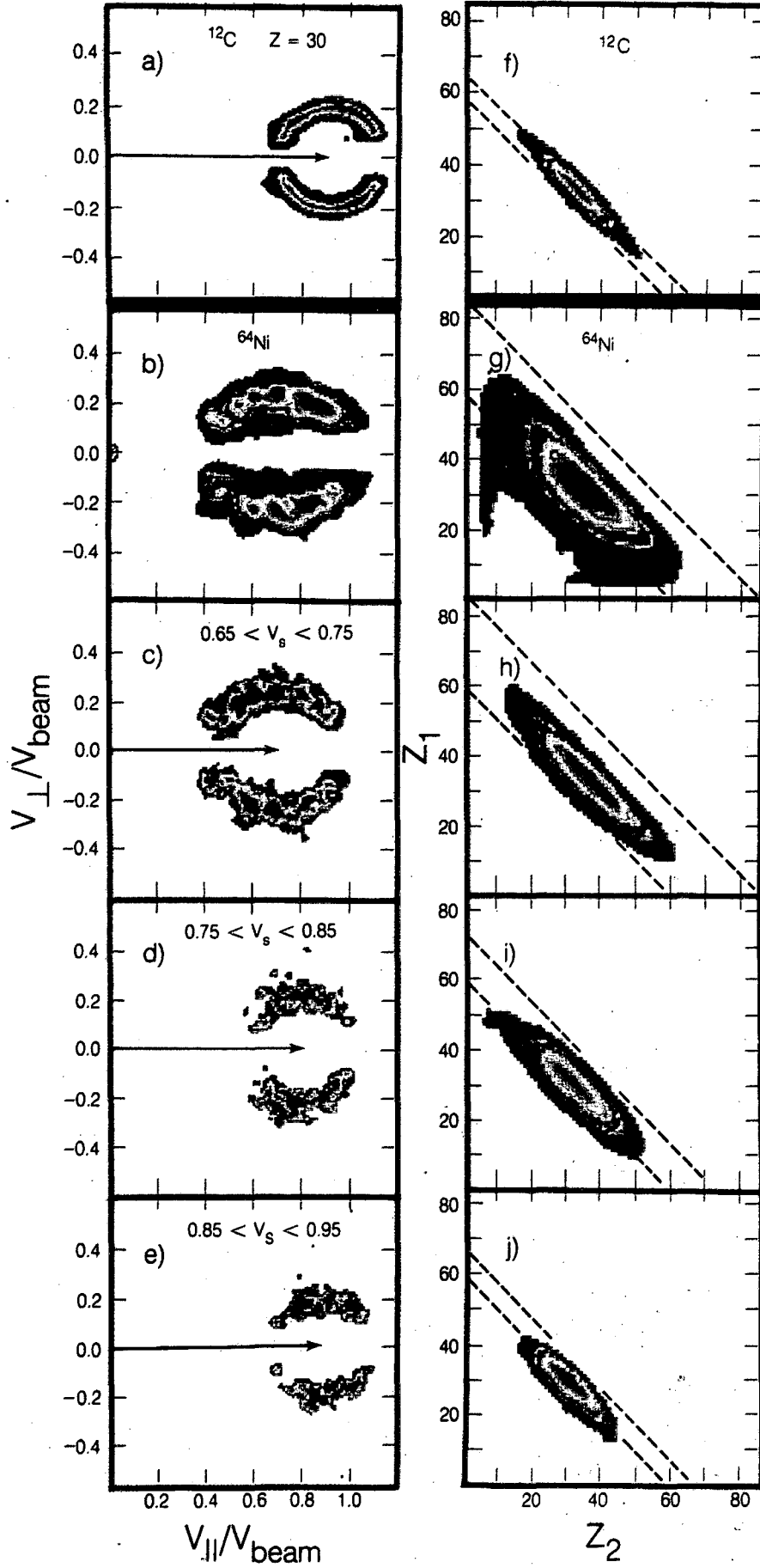
18 A MeV ^{139}La + ^{12}C, ^{64}Ni

Fig. 1

BBC 880-11279

$18 \text{ A MeV La} + {}^{12}\text{C}, {}^{27}\text{Al}, {}^{64}\text{Ni}$

$P(V_s/V_{beam})$

V_s/V_{beam}

${}^{12}\text{C}$

${}^{27}\text{Al}$

${}^{64}\text{Ni}$

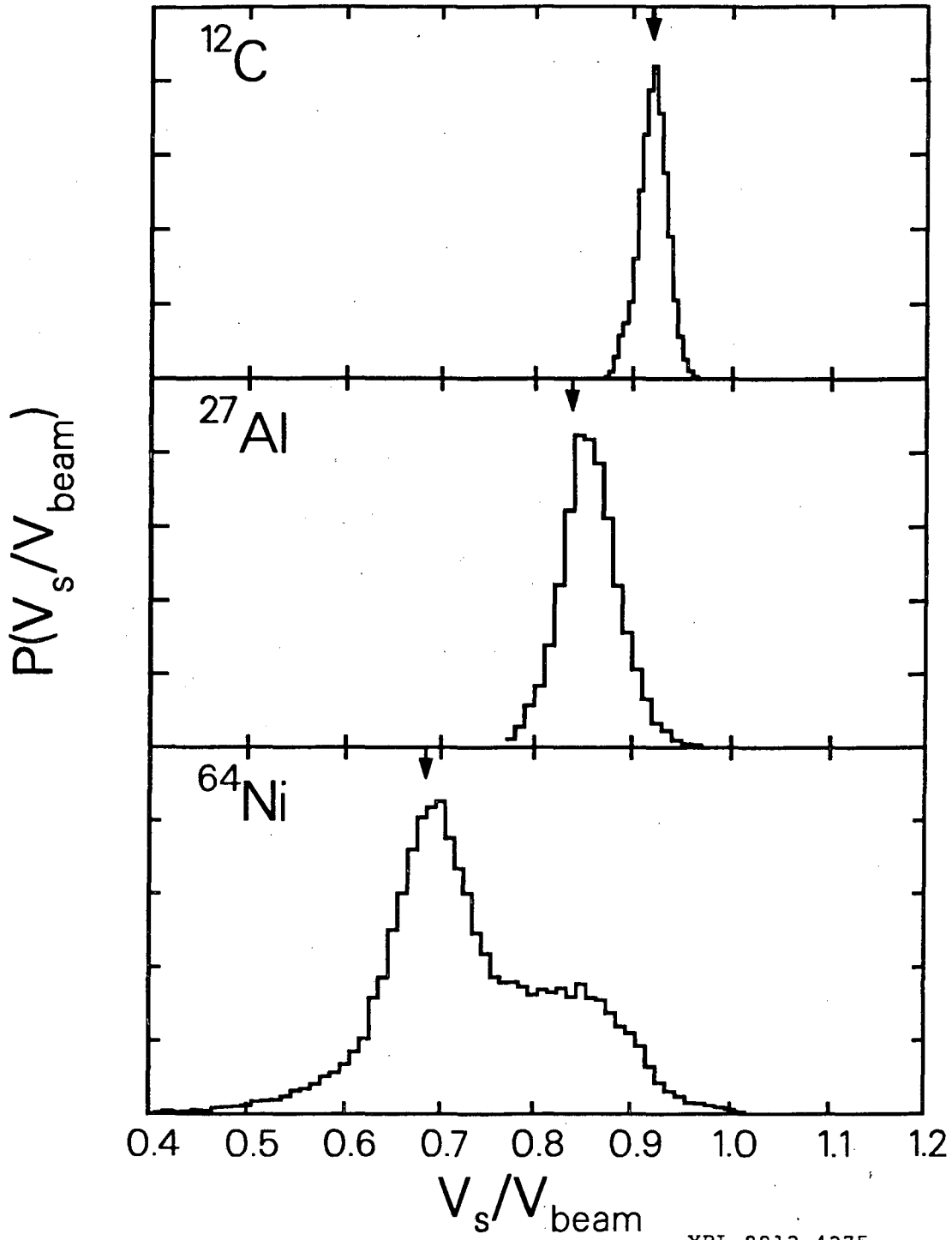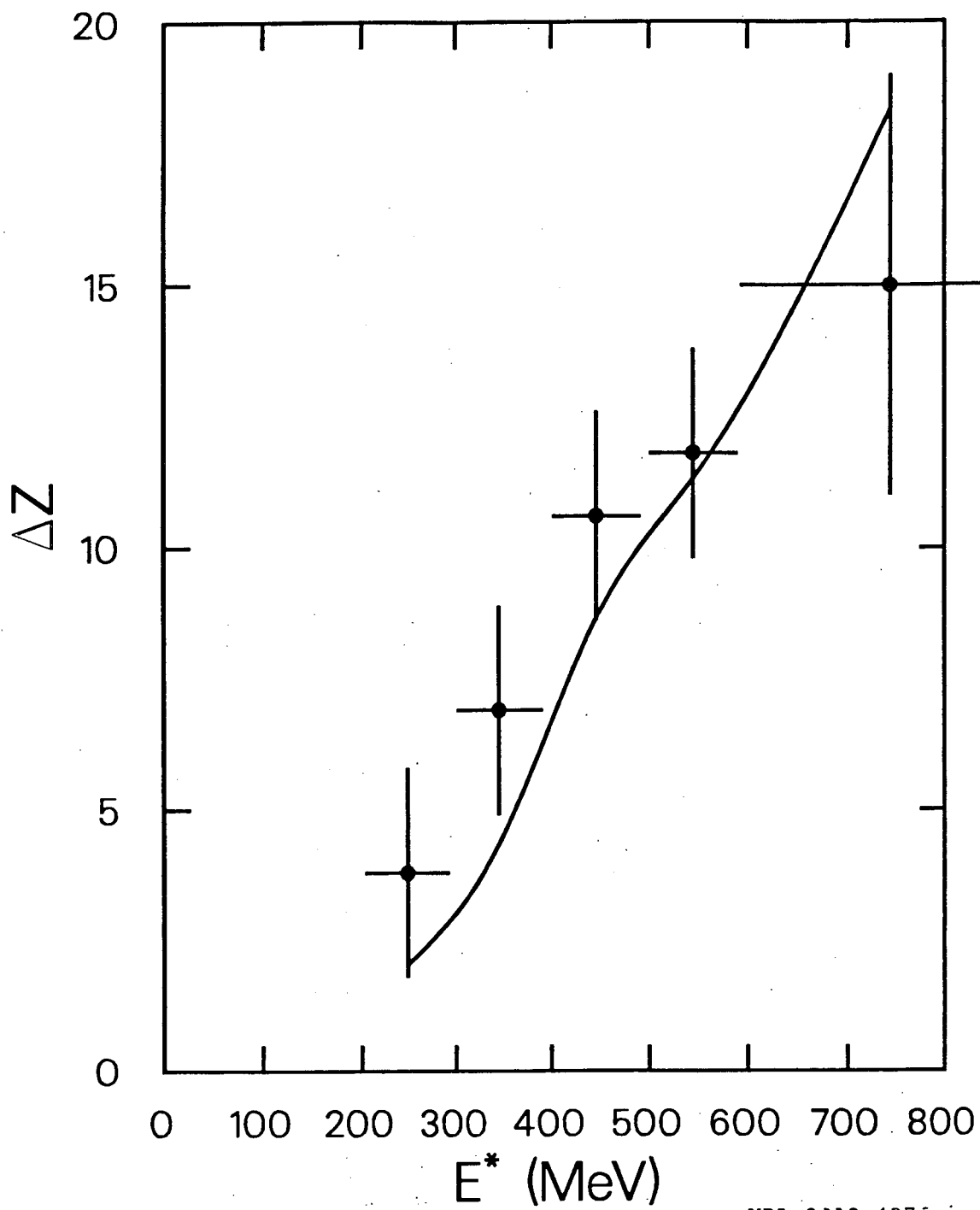0.4 0.5 0.6 0.7 0.8 0.9 1.0 1.1 1.2

XBL 8812-4275

Fig. 2

18 A MeV La + ^{64}Ni

XBL 8812-4276

Fig. 3

LAWRENCE BERKELEY LABORATORY
TECHNICAL INFORMATION DEPARTMENT
1 CYCLOTRON ROAD
BERKELEY, CALIFORNIA 94720